metals

MDPI

Article

An Investigation on the Softening Mechanism of 5754 Aluminum Alloy during Multistage Hot Deformation

Chang-Qing Huang [1,2,3,*], Jie Deng [1,3], Si-Xu Wang [1,2] and Lei-lei Liu [1,2]

1 State Key Laboratory of High-performance Complicated Manufacturing, Central South University, Changsha 410083, China; jiedeng@csu.edu.cn (J.D.); 143811002@csu.edu.cn (S.-X.W.); 153812016@csu.edu.cn (L.-l.L.)
2 Light Alloy Research Institute, Central South University, Changsha 410083, China
3 School of Mechanical and Electrical Engineering, Central South University, Changsha 410083, China
* Correspondence: huangcq64@csu.edu.cn; Tel./Fax: +86-8887-6183

Academic Editor: Hugo F. Lopez
Received: 12 January 2017; Accepted: 13 March 2017; Published: 23 March 2017

Abstract: Isothermal interrupted hot compression tests of 5754 aluminum were conducted on a Gleeble-3500 thermo-mechanical simulator at temperatures of 350 °C and 450 °C, and strain rates of 0.1 s^{-1} and 1 s^{-1}. To investigate the metadynamic recrystallization behavior, a range of inter-pass delay times (5–60 s) was employed. These tests simulated flat rolling to investigate how softening behaviors respond to controlled parameters, such as deformation temperature, strain rate, and delay times. These data allowed the parameters for the hot rolling process to be optimized. The dynamic softening at each pass and the effect of metadynamic recrystallization on flow properties and microstructural evolution were analyzed in detail. An offset yield strength of 0.2% was employed to calculate the softening fraction undergoing metadynamic recrystallization. A kinetic model was developed to describe the metadynamic recrystallization behaviors of the hot-deformed 5754 aluminum alloy. Furthermore, the time constant for 50% recrystallization was expressed as functions related to the temperature and the strain rate. The experimental and calculated results were found to be in close agreement, which verified the developed model.

Keywords: 5754 aluminum alloy; two-pass hot compression; dynamic softening; metadynamic recrystallization

1. Introduction

Different hot deformation processes of metals and alloys holds remarkable importance due to its direct effects on mechanical properties of final products. Therefore, the hot forming behavior of different materials has been a significant scientific issue [1]. The hot rolling and forging processes of aluminum alloy consist of several continuous deformation passes such as inter-pass periods between deformations. Materials will subject to static recovery, static recrystallization, and metadynamic recrystallization during the inter-pass periods [2]. Meanwhile, microstructural changes during multistage hot deformation render an effect on the mechanical characteristics of the metals and hence affect the deformation process. The manufacture of high quality products and optimization of pass schedules require a good knowledge of the relationships between hardening and softening behaviors. Modeling a kinetics equation necessitates a better understanding of the dynamic softening during hot deformation (simultaneous with straining) and the metadynamic or static softening between thermomechanical passes [3–6]. The modeling results are critical for the optimization of process parameters [7]. Generally, the degree of dynamic softening can be determined using relative softening (*RS*) or quasistatic softening, and four different methods, including offset-stress, back-extrapolation

stress, strain-recovery, and average stress methods, are employed to evaluate the softening fraction at the inter-pass durations.

A set of two-pass hot compression tests with various parameters were conducted in this study. These tests were designed to simulate flat rolling and provide in-depth insight into the high-temperature deformation behavior of 5754 aluminum alloy. The dynamic and metadynamic recrystallization softening behaviors of this studied alloy during multistage hot deformation were analyzed by relative softening (*RS*) and 0.2% offset-stress, respectively. To date, numerous studies have been directed to clarify the dynamic and metadynamic recrystallization behaviors of alloys and metals, and related kinetics equations have been developed [8–15]. No systematic work on, nor any fundamental knowledge of, multistage hot compression for this alloy has ever been reported. Accordingly, the present study has been designed to obtain 5754 aluminum alloys with good mechanical properties and to optimize its use for production. The purpose of this paper is mainly to focus on how metadynamic recrystallization softening behaviors respond to control parameters such as deformation temperature, strain rate, and delay time, thereby optimizing the hot rolling and forging process parameters. Moreover, a metadynamic recrystallization kinetics model of this aluminum alloy during two-pass deformation was established. Furthermore, the time constant for 50% recrystallization was expressed as functions related to the temperature and the strain rate. The experimental and calculated results were found to be in close agreement, which verified the developed model.

2. Materials and Material Testing

2.1. Materials

5754 aluminum alloy is a common Al–Mg alloy. Its mechanical properties, such as its moderate strength, its good corrosion resistance, its weldability, and its easy forming characteristics, have made it the primarily used material in the manufacture of doors, platform floors, body frames, and other structural components in the automotive industry. The experimental 5754 aluminum alloy used for multistage hot deformation tests were machined from a warm rolled plane. The chemical composition (wt %) of the alloy used in the experiments is reported in Table 1. The size of all specimens was 20 mm in the transverse direction, 18 mm in the normal direction, and 10 mm in the rolling direction (20 mm × 18 mm × 10 mm). The geometric outline of the deformation zone is approximated for rolling simulations. Figure 1 is given to show the specimens before forming, after one step, and after a second step of forming.

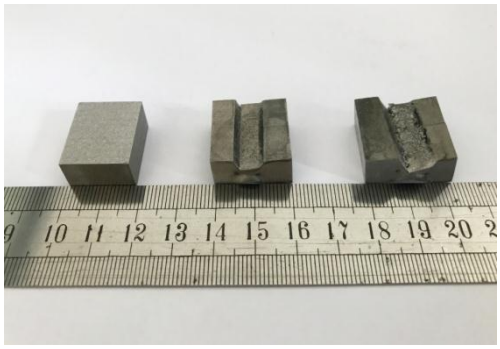

Figure 1. Specimens before forming, after one step, and after a second step of forming.

Table 1. The main composition of 5754 aluminum alloy (wt %).

Composition	Si	Cu	Mg	Zn	Mn	Gr	Al
Content (wt %)	0.40	0.10	2.6~3.6	0.20	0.50	0.30	Bal

2.2. Material Testing

A set of two-pass hot compression tests were conducted using a computer-controlled, servo-hydraulic Gleeble-3500 thermo-mechanical simulator. As can be observed in Figure 2, all specimens were heated at a rate of 10 °C/s to the specified temperature, then held at this temperature for 240 s to eliminate thermal gradients and to guarantee complete heating before compression. Tantalum foils were used to minimize the friction between the specimen and the indenter during compression. Two different forming temperatures (350 °C and 450 °C) and two strain rates (0.1 s^{-1} and 1 s^{-1}) were used. The deformation degree is the same in the two deformation passes, and a height reduction of 35% was adopted at each stage. The specimens would be held for times ranging from 5 s to 60 s at the deformation temperature during the inter-pass periods. In order to calculate the softening fraction, a second deformation pass was acquired.

During the hot compression process, the variations in strain and stress were continuously controlled by a computer, which was equipped with an automatic data acquisition system. The true stress–strain data were recorded by the testing system. To preserve the deformed microstructure, the specimens were quenched by cold water immediately after each compression experiment. The samples were cut along the direction of compression for analysis, and then mounted, polished, and anode-coated at 20 V for 2 min using a solution of fluoroboric acid (10 mL) in water (400 mL) for observation by optical microscopy. The strain distribution was concentrated in the center of the plane specimen, which assists the optical observation of the microstructures in the deformed material. Figure 3 shows optical microscopy images of the initial microstructures.

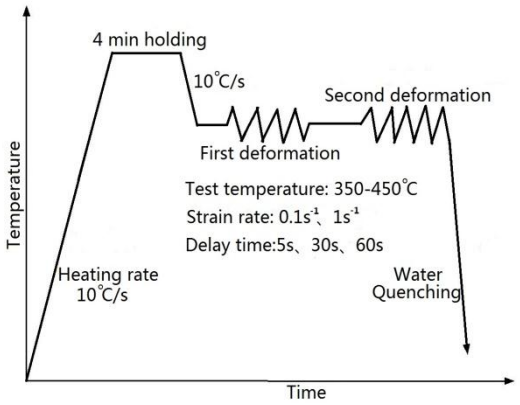

Figure 2. Experimental procedure for the two-pass hot compression tests.

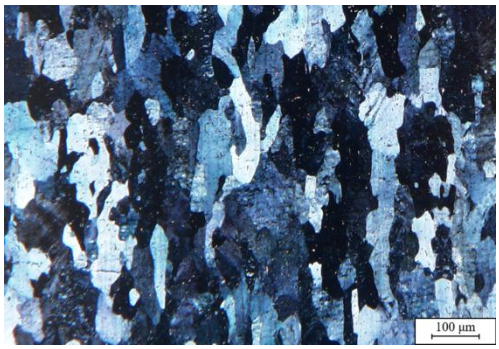

Figure 3. Initial microstructure of 5754 aluminum alloy.

3. Results and Discussion

3.1. Dynamic Softening Behavior

Aluminum alloys undergo mechanism restoration of dynamic recovery and dynamic recrystallization during deformation, particularly at high temperature. The flow behaviors are very complex during hot deformation, and the parameters of hot deformation, such as temperature and strain rate, affect the flow stress significantly. Therefore, the control of deformation parameters is critical in optimizing the final mechanical properties [16–20]. Figure 4 indicates the true representative stress–stain curves of the studied alloy under various deformation conditions. The stress level decreases with an increasing temperature or with a decreasing strain rate. These typical curves exhibit a single peak at a small strain, then decrease to a steady state, and remain constant at 350 °C at a strain rate of 1 s^{-1}, showing the dynamic softening behavior after peak stress. Generally, the yield stress at the second deformation stage decreases with an increasing delay time under the same temperature and the same strain rate. Verlinden et al. [21,22] proposed relative softening (*RS*) to quantify dynamic softening. The equation can be expressed as

$$RS = \frac{\sigma_p - \sigma_{p+0.25}}{\sigma_p} \quad (1)$$

where σ_p is the value of peak stress and $\sigma_{p+0.25}$ is the value taken at a strain of 0.25 beyond the peak (Figure 5). Dynamic hardening occurs as $RS < 0$, and dynamic softening occurs as $RS > 0$. The measured *RS* values (4.6%, 2.0%, 6.9%, and 5.2%) indicate that dynamic softening occurred here. The obtained stress–strain curves under all test conditions are single-peak without oscillation, which is an indication of softening behavior due to continuous dynamic recrystallization (CDRX) [23,24]. Furthermore, the *RS* values at the second deformation stage are smaller than those at the first. The inhomogeneous deformation and friction at high strain ($\varepsilon > 0.6$) lead to smaller *RS* values and to little dependence on delay times during inter-pass periods at the same temperature and the same strain rate. Those results signify that a dynamic softening fraction may approach zero with further straining at the second deformation stage.

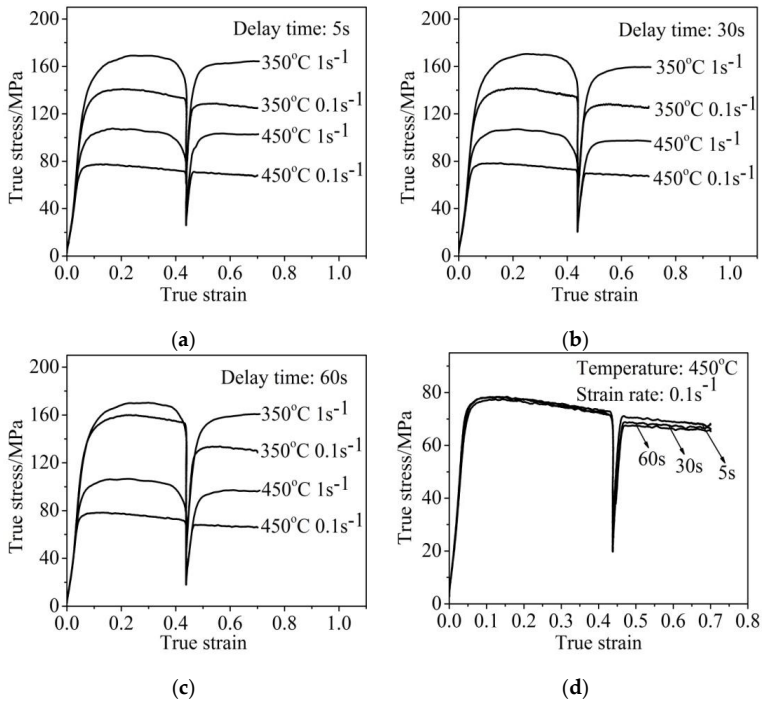

Figure 4. Typical true stress–strain curves of two-pass hot deformation under (**a**) delay time of 5 s; (**b**) delay time of 30 s; (**c**) delay time of 60 s; (**d**) temperature 450 °C and strain rate 0.1 s^{-1}.

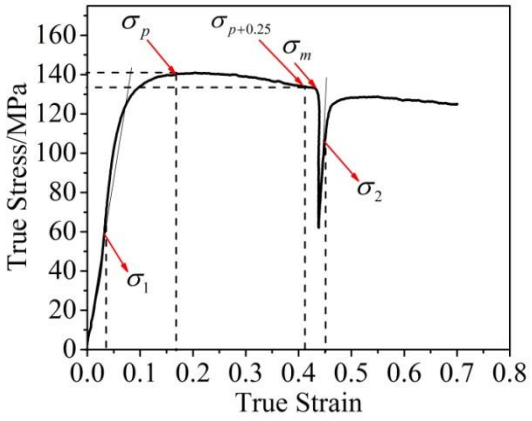

Figure 5. Determination of the characteristics stresses used to calculate softening fraction.

3.2. Modeling the Kinetics of Metadynamic Recrystallization

Softening mechanisms including static recovery, static recrystallization, and metadynamic recrystallization normally occur during inter-pass periods [25]. The degree of softening depend on the deformation temperature, strain rate, and holding time. Metadynamic recrystallization occurs when $\varepsilon > \varepsilon_c$, where ε is the strain at the interval and ε_c is the critical strain. Following this, in the present study, the metadynamic recrystallization appears to be the dominant softening mechanism during the inter-pass holding. The optical microscopy images at the center of the specimens after various inter-pass durations are shown in Figure 6. Coarse equiaxed alloy grains are evident in the initial microstructure of the alloy (Figure 3), and the topography appears primarily to be isometrically crystalline with a large angle. By contrast, the fine equiaxed recrystallized grains can be found for the two-pass compressed alloy. As can be seen, the microstructural evolution after a 30 s inter-pass delay time indicated full recrystallization. This observation is due to the fact that metadynamic recrystallization does not require an incubation period, and the softening process is relatively speedy. In this study, the softening fraction (*FS*) caused by metadynamic recrystallization can be quantitatively examined using 0.2% offset stress. The equation can be expressed as

$$FS = \frac{\sigma_m - \sigma_2}{\sigma_m - \sigma_1} \tag{2}$$

where σ_1 and σ_2 are the offset stresses at the first and second deformation stage, respectively, and σ_m is the flow stress at the interval (Figure 5).

The softening fraction is plotted against the delay time with various test parameters in Figure 7. As can be seen, the softening fraction of metadynamic recrystallization is increased by the inter-pass delay time. The stress–strain curves of the second pass will be the same as those of the first pass if the materials are fully softened during the inter-pass time. While no softening occurs, the second compression yields a stress–strain curve that is in accordance with the extrapolated one of the first stage. The amount of recrystallization significantly depends on the inter-pass delay time, and the softening fraction of metadynamic recrystallization is increased by the inter-pass delay time. As the delay time is reduced, a smaller amount of recrystallization occurs, which leads to a small amount of work hardening on reloading [26]. In addition, the softening fraction increases as the temperature increases due to the thermally activated softening mechanisms. The stored energy in the material at a high strain rate cannot be released as a consequence of lesser time being available at the first deformation stage, which can be released during the inter-pass periods and lead to the subsequent softening.

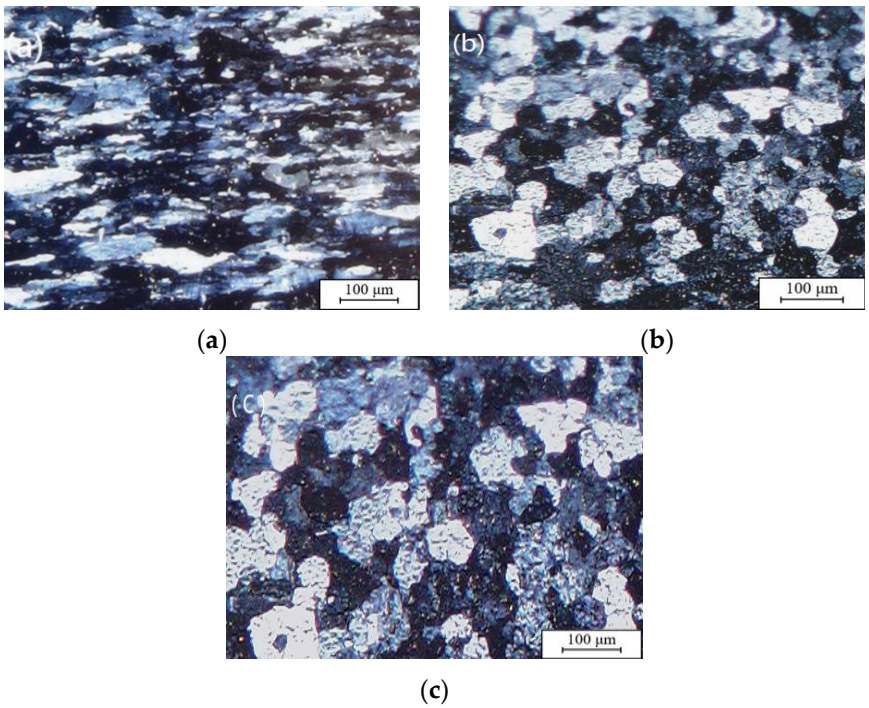

Figure 6. The optical microstructures after two-pass hot deformation for various inter-pass delay time of (**a**) 5 s, (**b**) 30 s, and (**c**) 60 s.

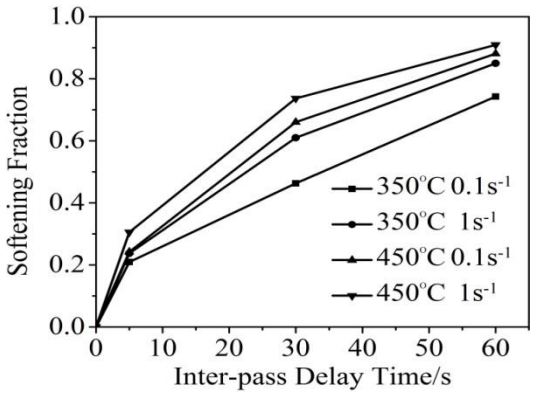

Figure 7. The curves of the softening fraction and the delay time.

The kinetics model of metadynamic recrystallization softening behavior can be expressed by the following exponent-type equation [27,28],

$$X_{mdrex} = 1 - \exp\left[-0.693\left(\frac{t}{t_{0.5}}\right)^{n}\right] \quad (3)$$

where X_{mdrex} is the softening fraction, and n is the Avrami exponent. $t_{0.5}$ is an empirical time constant for 50% recrystallization, which can be widely expressed as

$$t_{0.5} = a \times \dot{\varepsilon}^{m} \exp[Q_m/(RT)] \quad (4)$$

where a and m are material constants. R is the gas constant, which is equal to 8.314 J/(mol K). Q_m is the activation energy for recrystalliation. $\dot{\varepsilon}$ and T are the strain rate and the deformation temperature, respectively.

3.2.1. Determination of n

Taking the logarithm of Equation (3) of both sides,

$$\ln\left(\ln\left(\frac{1}{1-X_{mdrex}}\right)\right) = C + n\ln t \tag{5}$$

substituting the softening fraction X_{mdrex} and the related inter-pass delay time into Equation (5). Figure 8 shows the plot of $\ln\left(\ln\left(\frac{1}{1-X_{mdrex}}\right)\right)$ versus ln$t$. The average value of material constant n can be obtained by linear fitting, which is equal to 0.763.

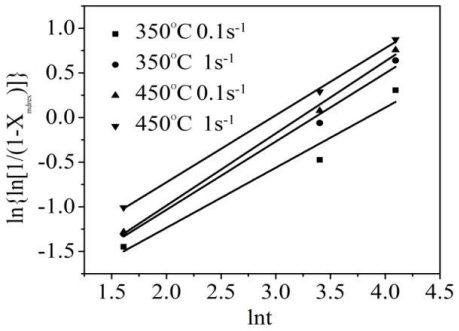

Figure 8. Relationship between $\ln\{\ln(1/(1-X_{mdrex}))\}$ and $\ln t$.

3.2.2. Determination of the Dependence of $t_{0.5}$ on Deformation Parameters

Taking the logarithm of Equation (4) of both sides,

$$\ln t_{0.5} = \ln X + m\ln\dot{\varepsilon} + \frac{Q_m}{RT} \tag{6}$$

substituting the value of $t_{0.5}$ and strain rate $\dot{\varepsilon}$ into the above equation. Material constant m and activation energy for metadynamic recrystallization Q can be obtained via linear fitting. Figure 9 shows a relationship between ln$t_{0.5}$ and ln$\dot{\varepsilon}$, as well as ln$t_{0.5}$ and $1/T$. The activation energy for metadynamic recrystallization Q is 18.045 KJ/mol. Much previous investigation has been focused on softening mechanisms during the inter-pass period of different aluminum alloys [2,29,30]. The exponent n and the present study is lower than that obtained for Al-5Mg and Al-9Mg alloy, i.e., n = 3.6 [30]. The variation of Avrami exponent n and activation energy Q values may be found for several reasons such as a decreasing growth rate or due to more planar growth morphology. In addition, the content of Mg will also lead to different activation energy for recrystallization.

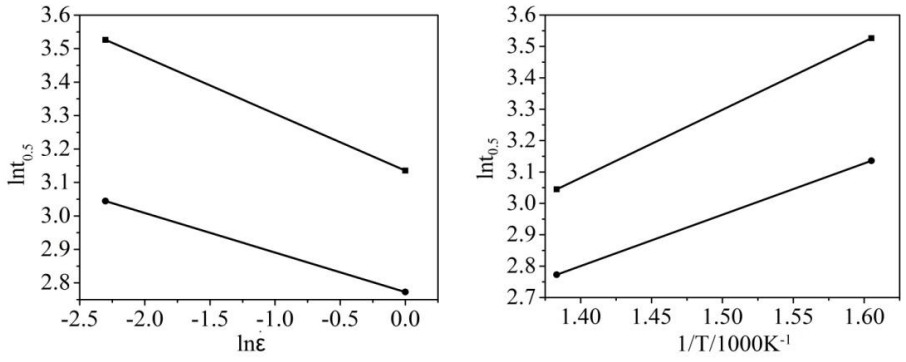

Figure 9. Relationship between (**a**) ln$t_{0.5}$ and ln$\dot{\varepsilon}$; (**b**) ln$t_{0.5}$ and $1/T$.

To conclude, the metadynamic recrystallization kinetic equation of two-pass hot-compressed 5754 aluminum can be assumed as:

$$X = 1 - \exp\left[-0.693\left(\frac{t}{t_{0.5}}\right)^{0.763}\right] \tag{7}$$

$$t_{0.5} = 0.698 \times \dot{\varepsilon}^{-0.1439} \exp[18045/(RT)] \tag{8}$$

3.3. Verification of the Developed Kinetic Equation

The softening behavior induced by metadynamic recrystallization during the two-pass hot deformation of 5754 aluminum alloy was investigated. The developed kinetic model has been verified by comparing the experimental and predicted metadynamic recrystallized fraction. Figures 10 and 11 illustrate the fitted experimental results using regression analysis, and most of the experimental and predicted softening fraction have a linear relationship and show good agreement with each other. Furthermore, the statistical parameters such as the correlation coefficient (R) and the average absolute relative error ($AARE$) were calculated to quantitatively verify the accuracy of the developed kinetic model. The correlative expressions are shown in Equations (9) and (10).

$$R = \frac{\sum_{i=1}^{N}(E_i - \overline{E})(P_i - \overline{P})}{\sqrt{\sum_{i=1}^{N}(E_i - \overline{E})^2 \sum_{i=1}^{N}(P_i - \overline{P})^2}} \tag{9}$$

$$AARE(\%) = \frac{1}{N}\sum_{i=1}^{N}\left|\frac{E_i - P_i}{E_i}\right| \times 100 \tag{10}$$

where E_i and P_i are the measured and calculated softening fraction, respectively. $\overline{E}$ and $\overline{P}$ are the average values of E_i and P_i, and N is the total number of the tested samples. The correlation coefficient is a reflection of the linear relationship between the experimental and predicted data. The $AARE$ is an unbiased statistical parameter used to evaluate the predictability of a model that can be calculated through a term-by-term comparison of relative error [31,32].

The values of R and $AARE$ were calculated to be 0.974 and 9.306%. The results indicate the model developed here is shown to provide accurate predictions for 5754 aluminum alloy.

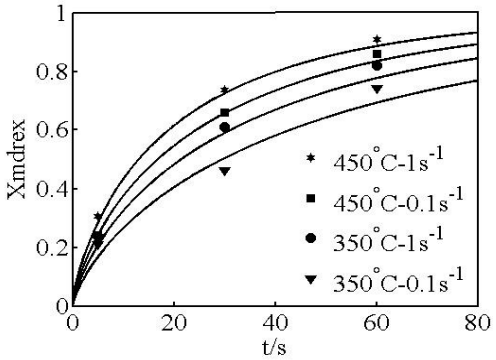

Figure 10. The comparison of the experimental and the calculated metadynamic softening fraction at different deformation temperatures.

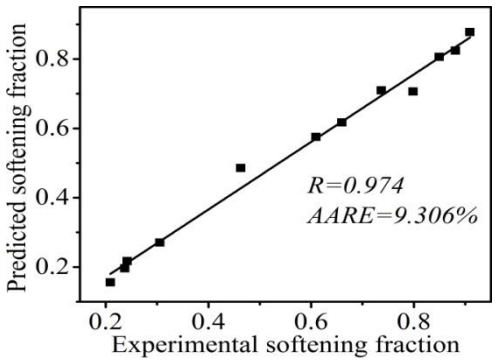

Figure 11. Comparison between the experimental and predicted softening fraction.

4. Conclusions

The current study was conducted to investigate the metadynamic recrystallization behavior of 5754 aluminum alloy via employing isothermal interrupted hot compression tests.

The degree of dynamic softening is quantified by relative softening, while the softening fraction due to metadynamic recrystallization is examined using the 0.2% off-stress method. A kinetics model of the studied alloy was developed here. A fundamental understanding of the metadynamic recrystallization allows for the processing variables to be controlled carefully in tandem hot rolling. The conclusions can be drawn as followed:

(1) The relative softening values under different test conditions signify the occurrence of dynamic softening at each stage, and the softening fraction may approach zero with further straining at the second deformation stage.

(2) For the two-pass hot compressed 5754 aluminum alloy, the restoration mechanism is governed by metadynamic recrystallization. The softening fraction attributed to metadynamic recrystallization increases with increasing deformation temperature, delay time, and strain rate.

(3) The predicted results were highly consistent with the experimental ones, which indicates that the developed kinetics equation can accurately describe the metadynamic recrystallization behaviors of 5754 aluminum alloy.

Acknowledgments: The authors appreciate financial support from the Natural Science Foundation of China under Grant 51275533 and by the State Key Laboratory of High-Performance Complex Manufacturing (Contract No. zzyjkt2013-10B), Central South University, China.

Author Contributions: Jie Deng conceived and designed the experiments; Chang-Qing Huang organized the research; Jie Deng performed the experiments; Chang-Qing Huang, Jie Deng, Si-Xu Wang, and Lei-lei Liu analyzed the data; Chang-Qing Huang wrote the manuscript; Jie Deng and Si-Xu Wang contributed to the revision of the paper.

Conflicts of Interest: The authors declare no conflict of interest.

References

1. Sang, D.; Li, Y. The Hot Deformation Activation Energy of 7050 Aluminum Alloy under Three Different Deformation Modes. *Metals* **2016**, *49*, 1–8. [CrossRef]
2. Lin, Y.C.; Li, L.T.; Xia, Y.C. A new method to predict the metadynamic recrystallization behavior in 2124 aluminum alloy. *Comput. Mater. Sci.* **2011**, *50*, 2038–2043. [CrossRef]
3. Zhou, M.; Clode, M.P. Constitutive equations for modeling flow softening due to dynamic recovery and heat generation during plastic deformation. *Mech. Mater.* **1988**, *27*, 63–76. [CrossRef]
4. Zhang, H.; Yang, L.B.; Peng, D.S.; Meng, L.P. Flow stress equation for multipass hot-rolling of aluminum alloys. *Cent. South Technol.* **2011**, *8*, 13–17. [CrossRef]
5. Zhang, H.; Yang, L.B.; Peng, D.S.; Meng, L.P. Recrystallization model for hot-rolling of 5182 aluminum alloy. *Trans. Nonferr. Met. Soc. China* **2011**, *11*, 382–386.

6. Sang, H.C.; Kim, S.I.; Yoo, Y.C. Determination of 'no-recrystallization' temperature of Invar alloy by fractional softening measurement during the multistage deformation. *Mater. Sci. Lett.* **1997**, *16*, 1836–1837.
7. Zheng, B.; Lin, Y.; Zhou, Y.; Lavernia, E.J. Gas Atomization of Amorphous Aluminum Powder: Part II. Experimental Investigation. *Metall. Mater. Trans. B* **2009**, *40*, 995–1004. [CrossRef]
8. Ding, H.L.; Wang, T.Y.; Yang, L.; Kamado, S. FEM modeling of dynamical recrystallization during multi-pass hot rolling of AM50 alloy and experimental verification. *Trans. Nonferr. Met. Soc. China* **2013**, *23*, 2678–2685. [CrossRef]
9. Xiang, S.; Liu, D.Y.; Zhu, R.H.; Jin-Feng, L.I.; Chen, Y.L.; Zhang, X.H. Hot deformation behavior and microstructure evolution of 1460 Al–Li alloy. *Trans. Nonferr. Met. Soc. China* **2015**, *25*, 3855–3864. [CrossRef]
10. Lin, Y.C.; Chen, M.S.; Zhong, J. Study of metadynamic recrystallization behaviors in a low alloy steel. *J. Mater. Process. Technol.* **2009**, *29*, 2477–2482. [CrossRef]
11. Lin, Y.C.; Chen, M.S.; Zhong, J. Study of static recrystallization kinetics in a low alloy steel. *Comput. Mater. Sci.* **2008**, *44*, 316–321. [CrossRef]
12. Shi, C.; Lai, J.; Chen, X.G. Microstructural Evolution and Dynamic Softening Mechanisms of Al-Zn-Mg-Cu Alloy during Hot Compressive Deformation. *Materials* **2014**, *7*, 244–264. [CrossRef]
13. Liu, Y.; Shao, Y.; Liu, C.; Chen, Y.; Zhang, D. Microstructure Evolution of HSLA Pipeline Steels after Hot Uniaxial Compression Microstructure Evolution of HSLA Pipeline Steels after Hot Uniaxial Compression. *Materials* **2016**, *9*, 721. [CrossRef]
14. Jiang, F.; Zhang, H.; Li, L.; Chen, J. The kinetics of dynamic and static softening during multistage hot deformation of 7150 aluminum alloy. *Mater. Sci. Eng. A Struct.* **2012**, *552*, 269–275. [CrossRef]
15. Maghsoudi, M.H.; Zarei-Hanzaki, A.; Changizian, P.; Marandi, A. Metadynamic recrystallization behavior of AZ61 magnesium alloy. *Mater. Des.* **2014**, *57*, 487–493. [CrossRef]
16. Zhang, P.; Yi, C.; Chen, G.; Qin, H.; Wang, C. Constitutive model based on dynamic recrystallization behavior during thermal deformation of a nickel-based superalloy. *Metals* **2016**, *6*, 1–19. [CrossRef]
17. Sun, Z.C.; Liu, L.; Yang, H. Microstructure evolution of different loading zones during TA15 alloy multi-cycle isothermal local forging. *Mater. Sci. Eng. A Struct.* **2011**, *528*, 5112–5121. [CrossRef]
18. Mandal, S.; Bhaduri, A.K.; Sarma, V.S. A study on microstructural evolution and dynamic recrystallization during isothermal deformation of a Ti-modified austenitic stainless steel. *Metall. Mater. Trans. A* **2011**, *42*, 1062–1072. [CrossRef]
19. Zhang, D.X.; Yang, X.Y.; Sun, H.; Li, Y.; Wang, J.; Zhang, Z.R.; Ye, Y.X.; Sakai, T. Dynamic recrystallization behaviors and the resultant mechanical properties of a Mg-Y-Nd-Zr alloy during hot compression after aging. *Mater. Sci. Eng. A Struct.* **2015**, *640*, 51–60. [CrossRef]
20. Agnoli, A.; Bernacki, M.; Logé, R.; Franchet, J.M.; Laigo, J.; Bozzolo, N. Selective Growth of Low Stored Energy Grains During δ Sub-solvus Annealing in the Inconel 718 Nickel-Based Superalloy. *Met. Mater. Trans. A* **2015**, *46*, 4405–4421. [CrossRef]
21. Verlinden, B.; Wouters, P.; McQueen, H.J.; Aernoudt, E.; Delaey, L.; Cauwenberg, S. Effect of homogenization and precipitation treatments on the hot workability of aluminum alloy AA2024. *Mater. Sci. Eng. A Struct.* **1900**, *123*, 239–245.
22. Verlinden, B.; Wouters, P.; McQueen, H.J.; Aernoudt, E.; Delaey, L.; Cauwenberg, S. Effect of different homogenization treatments on the hot workability of aluminum alloy AA2024. *Mater. Sci. Eng. A Struct.* **1900**, *123*, 229–237. [CrossRef]
23. Haghdadi, N.; Cizek, P.; Beladi, H.; Hodgson, P.D. A novel high-strain-rate ferrite dynamic softening mechanism facilitated by the interphase in the austenite/ferrite microstructure. *Acta Mater.* **2017**, *126*, 44–57. [CrossRef]
24. Liu, C.M.; Jiang, S.N.; Zhang, X.M. Continuous dynamic recrystallization and discontinuous dynamic recrystallization in 99.99% polycrystalline aluminum during hot compression. *Trans. Nonferr. Met. Soc. China* **2005**, *15*, 82–86.
25. Zhang, H.; Lin, G.Y.; Peng, D.S.; Yang, L.B.; Lin, Q.Q. Dynamic and static softening behaviors of aluminum alloys during multistage hot deformation. *J. Mater. Process. Technol.* **2004**, *148*, 245–249. [CrossRef]
26. Jung, K.H.; Lee, H.W.; Im, Y.T. A microstructure evolution model for numerical prediction of austenite grain size distribution. *Int. J. Mech. Sci.* **2010**, *52*, 1136–1144. [CrossRef]
27. Yue, C.X.; Zhang, L.W.; Liao, S.L.; Gao, H.J. Mathematical models for predicting the austenite grain size in hot working of GCr15 steel. *Comput. Mater. Sci.* **2009**, *45*, 462–466. [CrossRef]

28. Toloui, M.; Serajzadeh, S. Modelling recrystallization kinetics during hot rolling of AA5083. *J. Mater. Process. Technol.* **2007**, *184*, 345–353. [CrossRef]
29. Raghunathan, N.; Zaidi, M.A.; Sheppard, T. Recrystallization kinetics of Al-Mg alloys AA 5056 and AA 5083 after hot deformation. *Mater. Sci. Technol.* **1986**, *9*, 938–945. [CrossRef]
30. McQueen, H.J.; Ryum, N. Hot working and subsequent static recrystallization of Al and Al-Mg alloys. *Scand. J. Metall.* **1985**, *14*, 183–194.
31. Haghdadi, N.; Martin, D.; Hodgson, P. Physically-based constitutive modelling of hot deformation behavior in a LDX 2101 duplex stainless steel. *Mater. Des.* **2016**, *106*, 420–427. [CrossRef]
32. Haghdadi, N.; Zarei-Hanzaki, A.; Abedi, H.R. The flow behavior modeling of cast A356 aluminum alloy at elevated temperatures considering the effect of strain. *Mater. Sci. Eng. A Struct.* **2012**, *535*, 252–257. [CrossRef]